ORIGINAL PAPER

Antonio Doménech · Javier Alarcón

Electrochemistry of vanadium-doped tetragonal and monoclinic ZrO$_2$ attached to graphite/polyester composite electrodes

Abstract The electrochemistry of monoclinic and tetragonal vanadium-doped zirconias (VZrO$_2$), prepared from gel precursors with vanadium loadings ranging from 0.5 to 15 mol%, has been studied using abrasive-conditioned graphite/polyester composite electrodes immersed in aqueous HCl and HClO$_4$ solutions. Isolated vanadium centers form a solid solution in the zirconia lattice with a solubility limit close to 5 mol%. Above 5 mol%, finely dispersed V$_2$O$_5$ is formed. Vanadium centers located at the boundary sites of the zirconia lattice display successive one-electron transfer processes near to +0.25 and +0.10 V vs. SCE, whereas finely dispersed V$_2$O$_5$ yields three successive reduction processes at +0.46, +0.30, and +0.16 V vs. SCE. Electrochemical data indicate the presence of both V^{5+} and V^{4+} centers in the lattice of monoclinic and tetragonal zirconias, the V^{5+}/V^{4+} ratio decreasing as the vanadium loading increases.

Keywords Zirconia · Vanadium · Graphite · Polyester · Composite electrodes

Introduction

Vanadium-containing ZrO$_2$ systems that have been mainly used as ceramic pigments have recently claimed attention because of their catalytic properties [1, 2]. In spite of their wide use in the ceramics industry, there are some unsolved questions with regard to the structure of vanadium-containing zirconia yellow pigments. Thus,

A. Doménech (✉)
Departament de Química Analítica,
Universitat de València, Dr. Moliner 50,
46100 Burjassot (Valencia), Spain
E-mail: antonio.domenech@uv.es

J. Alarcón
Departament de Química Inorgànica,
Universitat de València, Dr. Moliner 50,
46100 Burjassot (Valencia), Spain

Booth and Peel [3] considered that a monomolecular thin film of V$_2$O$_5$ on the zirconia was responsible for the yellow color, but Ren et al. [4] claimed that the vanadium-containing ZrO$_2$ ceramic pigmenting system was a solid solution of V^{4+} in monoclinic ZrO$_2$. More recently, Tartaj et al. [5] attributed the observed color to the presence of V$_2$O$_5$ in the outer layers of the zirconia grains, with a small fraction of vanadium (ca. 15% of the total vanadium amount) entering as V^{4+} centers upon substitution of Zr^{4+} centers in the monoclinic zirconia lattice. In this context, prior works have shown evidence for V$_2$O$_5$ encapsulation in ZrO$_2$ when specimens were prepared from either colloidal or polymeric gels [6]. The formation of both tetragonal and monoclinic V^{4+}-containing ZrO$_2$ solid solutions was already observed for different compositions in the ternary V$_2$O$_5$-ZrO$_2$-SiO$_2$ system on heating gel precursors over the temperature range up to the formation of V^{4+}-ZrO$_2$ solid solutions [7]. More recently, tetragonal and monoclinic vanadium-containing zirconias (t-VZrO$_2$ and m-VZrO$_2$, respectively) have been prepared by gelling mixtures of zirconia and vanadia precursors, forming colloidal sols. Specimens were structurally characterized by X-ray powder diffraction and energy-dispersive X-ray microanalysis [8, 9]. A phase with the structure of tetragonal ZrO$_2$ was the first crystalline phase formed from the amorphous gel precursors containing different vanadium loadings. The formation of monoclinic vanadium-ZrO$_2$ solid solutions took place by phase transformation from the phase with the tetragonal structure. Electron paramagnetic resonance (EPR) spectroscopy and UV-Vis diffuse reflectance spectroscopy data, as well as data concerning the variation of lattice parameters as a function of vanadium loading, suggested that V^{4+} centers replace Zr^{4+} in hepta-coordinated sites of monoclinic zirconia [8] and octa-coordinated sites of tetragonal zirconia [9]. However, we have no definite evidence that all the incorporated vanadium in either tetragonal or monoclinic zirconia is tetravalent. Thus, it would be possible that, mainly for high vanadium loadings, the solid solution mechanism

also involved a combination of cation replacement and the formation of cation vacancies; i.e., Zr^{4+} may be not only isomorphously replaced by V^{4+}, but also by V^{5+} with the formation of cation vacancies. Furthermore, it is also evident that the amount of vanadium oxide, mainly in the glassy state, encapsulated into the zirconia grains should be increased as well. Accordingly, the presence and amount of vanadium oxide encapsulated into the zirconia lattice and the coexistence of an isomorphous substitution of Zr^{4+} centers by V^{4+} and V^{5+} remain as unsolved questions.

In order to investigate these problems, solid state electrochemistry can be used as a powerful methodology [10, 11, 12]. As recently described in detail by Scholz and Meyer [13], electrochemical data on solid microparticles attached to electrode surfaces are able to provide information concerning the oxidation state and the structural environment of electroactive centers. The electrochemistry of vanadium(V) oxide attached to carbon paste electrodes was studied in the 1970s by Lamache and Bauer [14]. The ability of vanadium oxides to undergo insertion reactions has motivated a continuous interest in their solid state chemistry because of the interesting electrical, optical, and magnetic properties of vanadium oxide phases [15, 16]. In particular, from the works of Brainina et al. [17], the electrochemistry of vanadium bronzes has been extensively studied in the context of solid state ionics owing to their use in batteries [18]. Recently, the electrochemistry of vanadium compounds at carbon paste electrodes with an electrolyte binder has been described by Barrado et al. [19], while the voltammetry of vanadium oxides in room temperature molten salts has been reported by Ryan and Riechel [20]. Scholz and co-workers [21] have compared the voltammetry of microcrystalline solid non-oxo- and oxovanadium(IV) complexes with the solution phase voltammetry of such complexes in dichloromethane. In the context of the chemistry of molecular sieves, the voltammetry of vanadium centers in vanadium silicate and vanadium aluminophosphate has been also recently reported by Sivasanker and co-workers [22]. The electrochemistry of vanadium species in aqueous solution has been recently treated by Privman and Hepel [23, 24] by studying the anodic and cathodic polarization of vanadium electrodes.

The purpose of the present work is to describe the electrochemical behavior of vanadium-containing ZrO_2 systems in comparison with those of vanadium oxide. This electrochemistry can be considered of interest in the field of solid state electrochemistry because a novel situation is obtained in which electroactive centers enter as doping agents into an electrochemically silent lattice. Accordingly, the electrochemistry of a series of monoclinic and tetragonal vanadium-containing ZrO_2 specimens with V/Zr molar ratios ranging from 0.000 to 0.150 has been studied.

Linear potential scan and differential pulse voltammetric responses of modified carbon paste electrodes and abrasive-conditioned glassy carbon and graphite/ polyester composite electrodes immersed in different aqueous media have been obtained and correlated with speciation and structural data.

Experimental

Preparation of vanadium-containing zirconia specimens

$V_xZr_{1-x}O_2$ gels, with $x = 0.000$, 0.005, 0.010, 0.015, 0.020, 0.025, 0.050, 0.075, 0.100, 0.125, and 0.150, were prepared, as previously reported [7], by gelling mixtures of zirconium n-propoxide $[Zr(OC_3H_7)_4]$, ZnP, and vanadyl acetylacetonate $(C_{10}H_{14}O_5V)$. The resulting $VO(acac)_2$ was dissolved in a mixture of acetylacetone (acacH) and n-propanol (n-PrOH) and kept under an argon atmosphere in a glovebox. Gelation occurred after adding water to the resulting solution and aging at 60 °C for several days. Gels were firstly dried in an open beaker for several days at room temperature and completely dried in a drying oven at 110 °C for 24 h. The dried gels displayed an orange color, the intensity depending on the amount of vanadium. The precursors were ground into powders using an agate mortar and pestle and then stepwise calcined up to 1300 °C with intermediate isothermal steps at several temperatures. After each heating, the sample was cooled in air in the furnace.

The whole reflectance spectra of t-$VZrO_2$ present a broad absorption charge-transfer band between 200 and 450 nm and two weak bands at 650 and 800 nm, while the reflectance spectra of m-$VZrO_2$ exhibit a broad and intense charge-transfer band between 220 and 500 nm with a weak band at 750 nm. In both cases, the bands at 650–800 nm are attributable to d-d electronic transitions associated with V^{4+} dissolved in the zirconia [8, 9]. The intensity of these bands increases as the vanadium loading increases, as also suggested by visual examination of the color of the samples.

Instrumentation

Linear potential scan voltammograms (LSVs) and differential pulse voltammograms (DPVs) were performed with a Metrohm E506 polarecord. Cyclic voltammograms were obtained with BAS CV 50 W equipment. Potential scan rates ranging from 1 to 500 mV/s were used. All electrochemical experiments were carried out at 298 K after immersion of the modified electrodes in well-deaerated solutions. $HCl + NaCl$ and $HClO_4 + NaClO_4$ were used as supporting electrolytes in total concentrations of 0.10–1.0 M. A standard three-electrode arrangement was used with a platinum auxiliary electrode and a saturated calomel reference electrode (SCE). The working electrode consisted of an abrasive-conditioned glassy carbon or composite electrode. Prior to a series of experiments the bare electrode was activated by applying +1.50 V vs. SCE for 10 min followed by –1.0 V for 1 min and then polished with a 0.1 μm alumina aqueous suspension on a polishing cloth prior to each run. This electrode treatment decreases background currents. To avoid possible sample contamination, a renewed supporting electrolyte solution was used for each probe.

Preparation of modified electrodes

Freshly prepared modified electrodes were used for all electrochemical measurements. Carbon/polyester composite electrodes were prepared using graphite powder (Aldrich, 1–2 μm size) and Estratil AL-100 polyester resin dissolved in styrene (33%) acting as reactive monomer. The co-polymerization reaction was catalyzed by cobalt octanoate incorporated in the initial prepolymer solution (0.07%) and initiated by adding ethyl methyl ketone peroxide (2%). The composite electrode was prepared by adding 45 wt% graphite to 55 wt% of freshly prepared polyester resin.

The samples were powdered in an agate mortar and pestle and placed on a glazed porcelain tile, forming a spot of finely distributed material. Abrasive conditioning of the samples was

performed, following Scholz and co-workers [13, 21], by pressing and vigorously rubbing the lower end of the electrode over that spot of sample. In all cases, the coatings examined contained 0.1–1.0 mg cm^{-2} of the dry material.

Materials

Zirconium n-propoxide and vanadyl acetylacetonate (Merck) were used as molecular precursors. Acetylacetone and n-propanol (Panreac) were used without further purification. V_2O_5 (Merck) and vanadyl acetylacetonate [$VO(acac)_2$, Aldrich] were used for blank experiments. Sodium perchlorate (Merck), sodium chloride (Merck), hydrochloric acid (Probus), acetic acid (Probus), and sodium acetate (Probus) were used to prepare the electrolyte solutions.

Results and discussion

Electrochemistry of V_2O_5

Figure 1 shows the cathodic (a) and anodic (b) LSVs for a V_2O_5-modified graphite/polyester composite electrode immersed in 0.10 M $HClO_4$. In the initial cathodic scan voltammogram, prominent but strongly overlapping cathodic peaks appear at $+0.46$ (C_1), $+0.30$ (C_2), and $+0.16$ V (C_3) vs. SCE, followed by an isolated peak near -0.55 V (C_4). In the anodic region, a well-defined oxidation peak appears at -0.30 V (A_1), followed by overlapping peaks at $+0.25$ (A_2), $+0.43$ (A_3), and $+0.85$ V (A_4). An identical response was obtained in HCl media. The voltammetric profile remains essentially unchanged upon variations of the potential scan rate between 10 and 200 mV/s. However, on increasing the pH of the solution, both in HCl + NaCl and $HClO_4$ + $NaClO_4$ electrolytes, the total area under the voltammetric peaks decreases whereas the peak C_1 progressively disappears, as can be seen in Fig. 2.

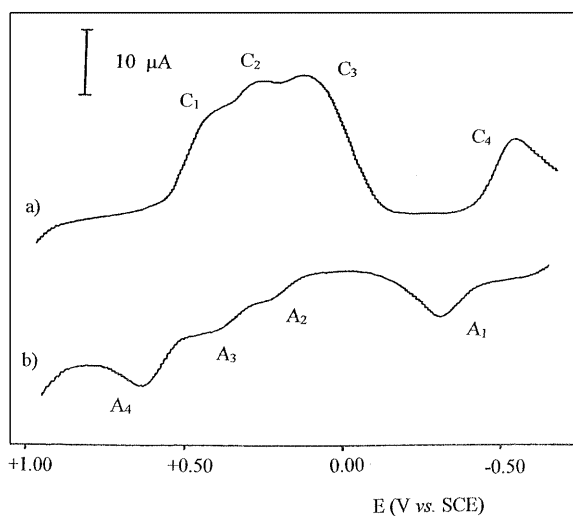In the initial anodic scans, weak oxidation signals are recorded. Upon repetitive cycling the potential scan, the anodic peak A_4 is enhanced while an additional cathodic peak near to $+0.65$ V (C_5) appears, as can be seen in Fig. 3a.

This voltammetry differs from that described for $NaVO_3$ and V_2O_5 attached to carbon paste electrodes that incorporate a conducting binder, for which isolated reduction peaks close to $+0.65$ and -0.55 V and isolated oxidation peaks at -0.35, $+0.45$, and $+0.90$ V have
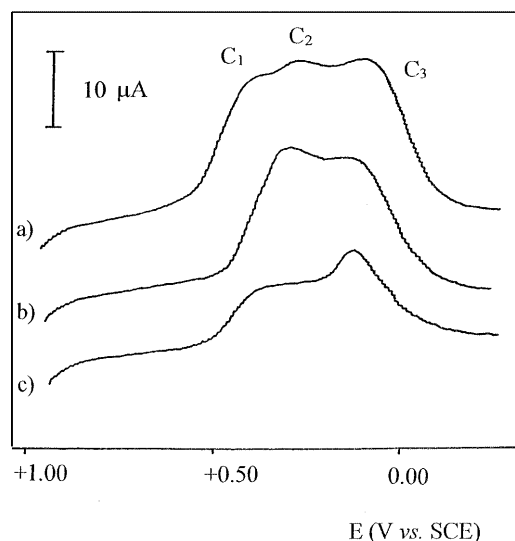
Fig. 2 Variation with pH of LSVs for V_2O_5 in HCl + NaCl (total conc. 0.10 M): (*a*) pH 1.0; (*b*) pH 2.0; (*c*) pH 3.0. Potential scan rate 10 mV/s
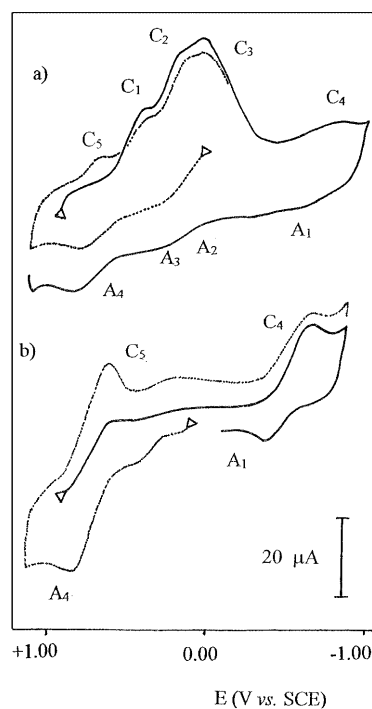
Fig. 1 LSVs for V_2O_5 in 0.10 M $HClO_4$: (*a*) cathodic scan; (*b*) anodic scan. Potential scan rate 10 mV/s

Fig. 3 Initial cathodic scan (*continuous lines*) and initial anodic scan (*dotted lines*) CVs for (*a*) V_2O_5 and (*b*) $VO(acac)_2$ in 0.10 M $HClO_4$. Potential scan rate 50 mV/s

been reported [19]. These differences can be rationalized, however, on considering the effect associated with the conducting binder that eases dissolution [25]. Thus, the potential of peak C_5 equals that reported by Barrado et al. [19] for the reduction of VO_2^+ ions in solution:

$$VO_{2(sol)}^+ + 2H^+ + e^- \rightarrow VO_{(sol)}^{2+} + H_2O \qquad (1)$$
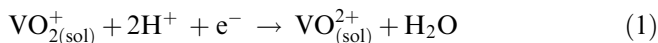
where the subscript (sol) represents species in solution.

Peak C_4 can be ascribed to the reduction of VO^{2+} ions in solution to V^{3+}, further reduced to V^{2+}. The peak potential recorded here agrees with that reported by Newton and Baker [26], the overall electrode reaction being:

$$VO_{(sol)}^{2+} + 2H^+ + 2e^- \rightarrow V_{(sol)}^{2+} + 2H_2O \qquad (2)$$
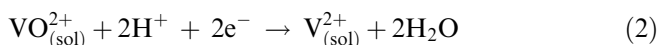
In agreement with this scheme, the potentials of peaks A_1 and A_2 are almost identical to those reported for the oxidation of vanadium species in solution, –0.35 and +0.45 V, respectively [19, 27, 28, 29], which can be described as:

$$V_{(sol)}^{2+} \rightarrow V_{(sol)}^{3+} + e^- \qquad (3)$$

$$V_{(sol)}^{3+} + H_2O \rightarrow VO_{(sol)}^{2+} + 2H^+ + e^- \qquad (4)$$
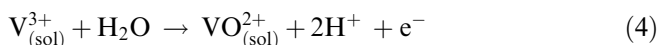
Consistently, the peak potential recorded here for A_4 agrees with that reported by Barrado et al. [19] for the oxidation of VO^{2+} ions in solution (+0.85 V). This process can be represented by the reverse of Eq. 1.

To corroborate this scheme, the electrochemical response of V_2O_5 can be compared with that of VO (acac)$_2$-modified electrodes. As can be seen in Fig. 3, the initial anodic scan CVs of VO(acac)$_2$ present a prominent oxidation peak at +0.85 V (A_4) which is followed, in the subsequent cathodic scan, by a reduction peak at +0.60 V (C_5) corresponding to the VO_2^+/VO^{2+} couple previously described. In initial cathodic scan CVs the reduction peak at –0.55 V (C_4) appears, corresponding, as before, to the reduction of VO^{2+} ions in solution.

Accordingly, peaks C_1–C_3 recorded in V_2O_5-modified composite electrodes are attributable to solid species attached to the electrode surface. As depicted in Fig. 3, upon repetitive cycling the potential scan, the intensity of cathodic peaks C_1, C_2, and C_3 decreases while that of anodic peaks A_2 and A_3 increases. Couples C_5/A_4 and C_4/A_1, attributed to species in solution, are also progressively enhanced on repetitive cyclic voltammetry.

The most prominent processes, C_1 and C_2, can be described as a reductive dissolution of vanadium(V) oxide following the scheme reported for, among others, lead [10, 11, 13], iron [30, 31, 32, 33], and manganese [34] oxides:

$$V_2O_5 + 4H^+ + 2e^- \rightarrow 2VO_{(sol)}^{2+} + 2H_2O \qquad (5)$$
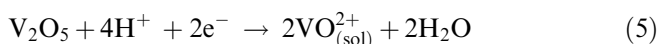
superimposed on a solid state redox process that presumably parallels that described for manganese dioxide [34, 35, 36, 37]:

$$V_2O_5 + 2H^+ + 2e^- \rightarrow V_2O_4 + H_2O \qquad (6)$$

This is followed by the reductive dissolution of such vanadium oxide (peak C_3):

$$V_2O_4 + 8H^+ + 2e^- \rightarrow 2V_{(sol)}^{3+} + 4H_2O \qquad (7)$$
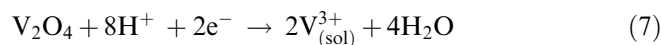
This scheme is consistent with the fast decay of the current after each voltammetric peak, which can be seen on comparing the diffusive region of peak C_3 with that of peak C_4 in Fig. 1, and the presence of a well-defined oxidation peak A_3 in anodic scans which would be interpreted as the anodic counterpart of the process represented by Eq. 6.

Accordingly, the oxidation peak near to +0.45 V (A_3) can be described in terms of an oxidative dissolution of V(IV) species comparable to that of chromium oxide [33]:

$$V_2O_4 \rightarrow 2VO_{2(sol)}^+ + 2e^- \qquad (8)$$

The electrochemical mechanism, however, is complicated, as can be seen in the DPV depicted in Fig. 4, in which the peak C_3 appears as a complicated two-peak system preceded by a shoulder.

Electrochemistry of vanadium-doped zirconia

Figure 5 compares the CVs of (a) t-VZrO$_2$ and (b) m-VZrO$_2$, both containing a 0.050 V/Zr molar ratio in 0.10 M HCl. Initial cathodic scan CVs for t-VZrO$_2$ show well-defined cathodic peaks at +0.35 (C_6) and +0.12 V (C_7), preceding peak C_4 at –0.53 V. In the subsequent anodic scan, the anodic peak A_1 is followed by well-defined oxidation peaks at +0.18 (A_5) and +0.41 V (A_6). Upon repetitive voltammetry, peaks C_6 and C_7 decrease while peaks A_5 and A_6 increase. In initial anodic scan CVs, also depicted in Fig. 5, peak A_5 is almost entirely absent, while peak A_6 is weaker than that obtained after a
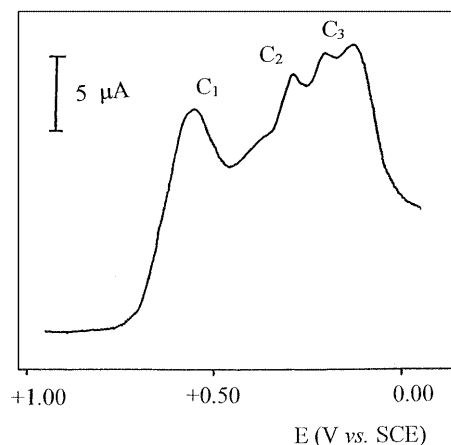

Fig. 4 Cathodic DPV for a V_2O_5-modified graphite/polyester composite electrode in 0.10 M HCl. $v = 10$ mV/s; $\Delta U = 80$ mV
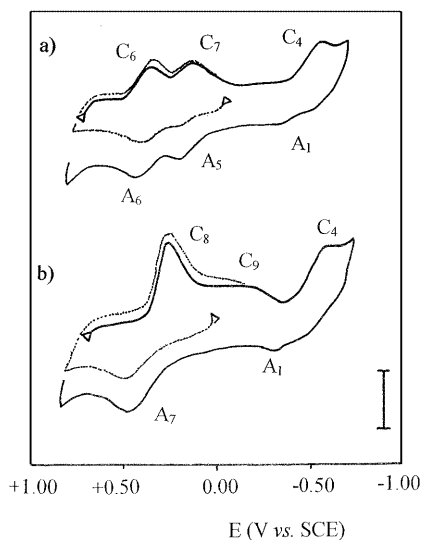
Fig. 5 Initial cathodic scan (*continuous lines*) and initial anodic scan (*dotted lines*) CVs for (*a*) t-VZrO$_2$ ($x=0.01$) and (*b*) m-VZrO$_2$ ($x=0.01$) immersed in 0.10 M HCl. Potential scan rate 20 mV/s

prior reductive step. In the subsequent cathodic scan, peaks C$_6$ and C$_7$, however, become well defined.

Initial cathodic scan CVs for m-VZrO$_2$ exhibit only one well-defined cathodic peak at +0.25 V (C$_8$), followed by an ill-defined shoulder at –0.20 V (C$_9$) and the ubiquitous peak C$_4$ at –0.53 V. In the reverse scan, peak A$_1$ is followed by only one well-defined anodic peak at +0.47 V (A$_7$). As in the case of t-VZrO$_2$, upon repetitive cycling the potential scan, cathodic peaks C$_8$ and C$_9$ slowly decrease, while peak A$_7$ increases. In initial anodic scan CVs, peak A$_7$ becomes ill defined and followed by the well-defined peak C$_8$.

As expected, blank electrodes modified with zirconias not containing vanadium ions ($x=0.00$) are electrochemically silent in this potential region, denoting that all these peaks are attributable to electrochemical processes involving vanadium species. Similar results were obtained in HCl + NaCl and HClO$_4$ + NaClO$_4$ electrolytes, the pH ranging from 0.0 to 3.0.

The voltammetric response, however, varies with the V/Zr ratio, as can be seen in Fig. 6 for t-VzrO$_2$. On increasing the V/Zr ratio, the voltammograms become increasingly similar to those for V$_2$O$_5$ and the peak currents are progressively enhanced. Thus, for V/Zr ratios larger than 0.05, LSVs consist of three cathodic peaks and three anodic peaks (Fig. 6a, b) with a voltammetric profile close to that displayed by vanadium(V) oxide (see Fig. 3). On decreasing the V/Zr ratio below $x=0.05$, only the well-defined peaks C$_6$, C$_7$, A$_5$, and A$_6$ remain (Fig. 6c).

Similar results were obtained for m-VZrO$_2$, with three overlapping couples for V/Zr ratios larger than 0.05 (see Fig. 7a, b). Below $x=0.05$, only the peaks C$_8$ and A$_7$ remain well developed, as illustrated in Fig. 7c.

According with the above results, it can be assumed that the limit of solubility of vanadium in both
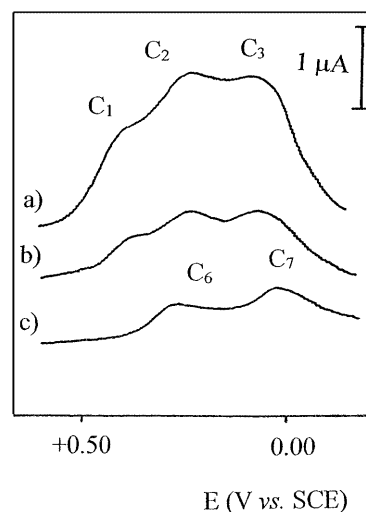

Fig. 6 Cathodic LSVs for t-VZrO$_2$ in 0.10 M HCl: (*a*) $x=0.150$; (*b*) $x=0.075$; (*c*) $x=0.005$. Potential scan rate 20 mV/s
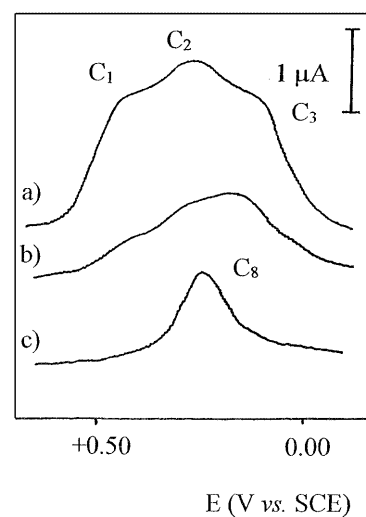

Fig. 7 Cathodic LSVs for m-VZrO$_2$ in 0.10 M HCl: (*a*) $x=0.150$; (*b*) $x=0.075$; (*c*) $x=0.005$. Potential scan rate 20 mV/s

monoclinic and tetragonal zirconia is close to $x=0.05$. These results confirm previous findings obtained by means of a combination of measurements from spectroscopic, diffraction, and microscopy techniques [8, 9].

To analyze this electrochemical response it should be noted that vanadium ions can exist in the zirconia matrix as isolated ions substituting zirconium ions in the crystal lattice, isolated ions in defect sites, and as a finely dispersed oxide phase on the outer surface of zirconia crystals. Then, electron transfer processes in vanadium-containing zirconia can be described in terms of the coexistence of (1) processes affecting vanadium ions at the boundary of the zirconia matrix, or (2) processes involving dispersed vanadium oxide.

The observations previously described on the variation of the voltammetric response with the V/Zr molar ratio suggest that the proportion of finely dispersed

vanadium(V) oxide increases significantly as the vanadium loading increases. Then, the electrochemical response of t-VZrO$_2$ and m-VZrO$_2$ materials with low loadings of vanadium must be representative of V^{4+} (and/or V^{5+}) centers substituting Zr^{4+} centers in the zirconia lattice. Accordingly, peaks C$_6$ and C$_7$ of t-VZrO$_2$ and peak C$_8$ of m-VZrO$_2$ are representative of vanadium centers inserted into the zirconia lattice. The electrochemistry of such centers differs from that of solid V$_2$O$_5$. Thus, as can be seen in Fig. 8, the peak potential for peak C$_1$ in vanadium(V) oxide is negatively shifted on increasing the potential scan rate, while the peak potentials of peaks C$_6$ and C$_7$ of t-VZrO$_2$ and the peak C$_8$ for m-VZrO$_2$ become essentially constant in the studied range of potential scan rates. This behavior refers to a thin-layer response which would be associated with a set of electroactive centers attached to a non-conducting, non-reactive bulk.

The foregoing considerations are supported by Tafel analysis of the rising portion of the voltammetric curves depicted in Fig. 9. The peak C$_1$ for vanadium oxide shows a linear dependence of log(i) on the applied potential, with a slope of 0.0120 mV^{-1} (line A). For t-VzrO$_2$ (peak C$_6$) and m-VZrO$_2$ (peak C$_8$) with $x = 0.05$, Tafel plots present two differentiated regions, with slopes of 0.0064 and 0.0176 mV^{-1}, suggesting that two different electrode processes are superimposed (lines B and D). On decreasing the vanadium loading, Tafel plots tend progressively to a single straight line with a slope of 0.064 mV^{-1}, as illustrated by lines C, D, and E in Fig. 9, corresponding to t-VZrO$_2$ (peak C$_6$) with $x = 0.10$, 0.005, and 0.010, respectively.

Peak potentials for processes C$_6$–C$_8$ and A$_5$–A$_7$ vary linearly with the pH in the 0–3.5 pH range, with slopes near to 95 mV. This suggests that proton transfer reactions are involved in the electron transfer process. Interestingly, the peaks C$_6$–C$_8$ and A$_5$–A$_7$ exhibit sharp
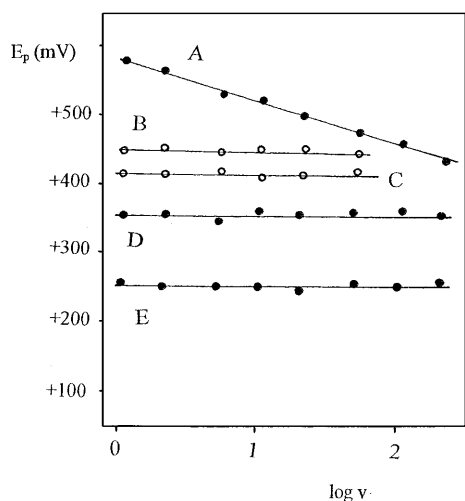
and symmetric profiles, close to that characteristic of electrode processes involving electroactive species strongly attached to the electrode surface. Tentatively, reduction processes C$_6$–C$_8$ can be described in terms of electron transfer steps in which charge conservation requires the insertion of protons or positive ions into the lattice coupled with the electron transfer process, following the scheme proposed for zeolite-attached ions [38, 39] and for vanadium-containing molecular sieves [22]. Accordingly, the electrode processes C$_6$ and C$_8$ can represented by:

$$[ZrO_2]V^{5+}_{(b)} + M^+_{(sol)} + e^- \rightarrow [ZrO_2]V^{4+}_{(b)} + M^+_{(b)} \qquad (9)$$
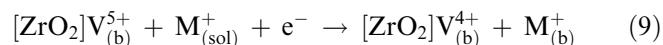
where the subscript (b) denotes the boundary of the zirconia grains and M$^+$ represents a proton or a charge-compensating ion of the electrolyte solution. This is consistent with the observed absence of peaks C$_1$–C$_3$ in the LSVs of vanadium-doped zirconias having low vanadium loadings. As can be seen in Fig. 5, the couples C$_6$/A$_6$ and C$_7$/A$_5$ for t-VZrO$_2$ and C$_8$/A$_7$ for m-VZrO$_2$ remain stable upon repetitive cycling the potential scan. The observed differences in the height of the cathodic and anodic peaks in potential scans initiated cathodically and anodically can be explained (1) on assuming that different amounts of V^{5+} and V^{4+} coexist initially in the zirconia, and (2) on assuming that only V^{5+} exists initially in the zirconia lattice. In this second case, V^{5+} centers should be entirely reduced to V^{4+} but only a limited fraction of this should be re-oxidized in anodic scans to V^{5+}.

Current data act in support of hypothesis (1), in view of the observed cycling stability of all cathodic and anodic peaks. Additionally, prior spectral and EPR data appear to indicate that both V^{5+} and V^{4+} centers exist in the studied systems [8, 9]. In particular, the intensity of the absorption bands at 650 and 800 nm for t-VZrO$_2$ and that at 750 nm for m-VZrO$_2$, all assigned to V^{4+} centers, increase significantly as the vanadium loading increases. Spectral data suggest that the population of
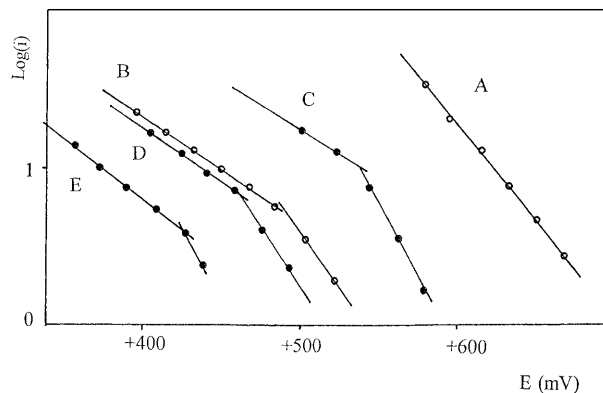

Fig. 8 Variation of peak potentials on the potential scan rate for A V$_2$O$_5$, peak C$_1$; B t-VZrO$_2$ ($x = 0.05$), peak C$_6$; C t-VZrO$_2$ ($x = 0.05$), peak C$_7$; D m-VZrO$_2$ ($x = 0.05$), peak C$_8$. Electrolyte: 0.10 M HCl

Fig. 9 Tafel plots from the rising portion of LSVs ($v = 20$ mV/s) for A V$_2$O$_5$ (peak C$_1$); B m-VZrO$_2$ ($x = 0.05$), peak C$_8$; C t-VZrO$_2$ ($x = 0.10$), peak C$_6$; D t-VZrO$_2$ ($x = 0.05$), peak C$_6$; E t-VZrO$_2$ ($x = 0.01$), peak C$_6$. Electrolyte: 0.10 M HCl

V^{4+} centers relative to V^{5+} ones is enhanced as the total vanadium loading increases.

Accordingly, the electrochemical oxidation of vanadium centers in zirconias can be represented as:

$$[ZrO_2]V^{4+}_{(b)} + M^+_{(b)} \rightarrow [ZrO_2]V^{5+}_{(b)} + M^+_{(sol)} + e^- \quad (10)$$
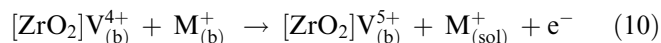
The absence of peak A_4 for both m-VZrO$_2$ and t-VZrO$_2$ is indicative that there are no oxidative dissolution processes and that the electrochemical process described by Eq. 10 is operative in these systems. Finally, peaks C_7 and C_9 must correspond to the subsequent reduction of boundary-associated V^{4+} centers yielding V^{3+} ions in solution, following a reductive dissolution scheme similar to that previously described for vanadium oxide. This results in the subsequent appearance of peak C_4, as shown in Fig. 5.

Taking into account the foregoing considerations, the differences in the observed electrochemical response of tetragonal and monoclinic zirconias can be attributed to electron transfer processes affecting vanadium species existing at the boundary of the zirconia matrix with different coordination environments. This is in agreement with the results reported for vanadium silicates containing vanadium centers having square pyramidal and tetrahedral coordinations [22].

It should be noted that in V_2O_5 there is a strongly distorted octahedral coordination of vanadium ions that can be described in terms of a five-coordination (square pyramidal) environment [40], with V–O bond lengths of 1.59, 1.78, 1.88 (two), and 2.02 Å. In monoclinic zirconia, Zr^{4+} ions are seven-coordinated with three oxygen atoms at 2.07 Å, and four oxygen atoms at 2.21 Å. In tetragonal zirconia, although each Zr^{4+} ion is eight-coordinated, there are two distinct groups of oxygen atoms, four at 2.065 Å and four at 2.455 Å [40]. Accordingly, the observed differences in the electrochemistry of t-VZrO$_2$ and m-VZrO$_2$ should reflect the existence of different coordinative arrangements for electroactive vanadium centers in the zirconias.

Taking into account the foregoing considerations, the voltammetric data can provide a direct estimate of the relationship between the amounts of vanadium existing as a finely dispersed vanadium(V) oxide and that isomorphously substituting Zr^{4+} centers in the boundary of zirconia lattices. In addition, one can estimate the V^{5+}/V^{4+} ratio for vanadium centers located in reticular positions in the zirconia lattice. For these purposes, the area of the voltammetric peaks was determined. As can be seen in Fig. 10a, for doped zirconias containing low amounts of vanadium ($x < 0.05$), the total area of the cathodic peaks increases almost linearly with the molar fraction of vanadium. However, for $x > 0.05$ the area increases more rapidly, suggesting that finely dispersed vanadium(V) oxide, which is more accessible electrochemically than vanadium centers in the zirconia lattice, are present in increasing amounts. Assuming that the molar fraction of isomorphously substituted vanadium increases until it apparently tends to a limiting value

(dotted line in Fig. 10a), the amount of vanadium existing as finely dispersed vanadium oxide can be estimated by subtracting the total peak area from the peak area for reticular vanadium.

The quotient V^{5+}/V^{4+} in vanadium centers isomorphously substituting Zr^{4+} ions can be estimated on comparing the areas for anodic peaks A_6 (for t-VZrO$_2$) and A_7 (for m-VZrO$_2$), measured in the first scan of the LSVs initiated anodically at 0 V, and cathodic peaks C_6 (for t-VZrO$_2$) and C_8 (for m-VZrO$_2$), measured in the first scan of the LSVs initiated cathodically at +0.8 V, after subtracting the contribution of finely dispersed V_2O_5. Figure 10b shows a representation of the ratios (A_6 peak area)/(C_6 peak area) for t-VZrO$_2$ and (A_7 peak area)/(C_8 peak area) for m-VZrO$_2$, all corrected by subtracting the contribution of V_2O_5 illustrated in Fig. 10a. These provide an estimate of the (reticular V^{5+})/(reticular V^{4+}) ratio for t-VZrO$_2$ and m-VZrO$_2$. The results depicted in Fig. 10b clearly indicate that the V^{5+}/V^{4+} ratio in doped zirconias increases as the total vanadium loading decreases. This is possibly due to the existence of a limited amount of vacancies in the ZrO$_2$
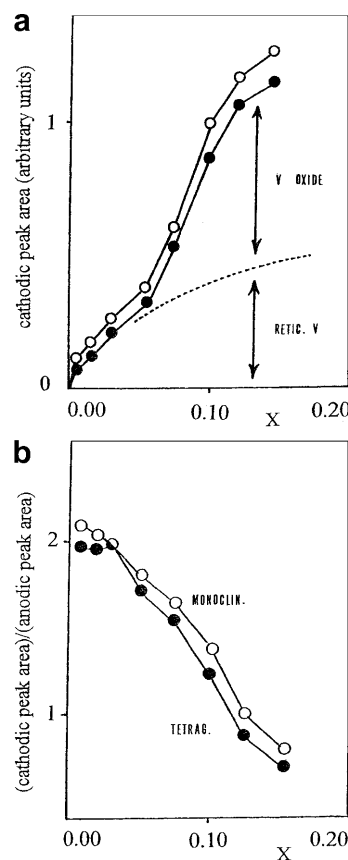

Fig. 10a, b Analysis of the dependence of peak areas on the nominal molar fraction of vanadium in t-VZrO$_2$ (*solid circles*) and m-VzrO$_2$ (*open circles*). **a** Total cathodic peak area with estimated reticular vanadium (*dotted line*); **b** quotient between the cathodic and anodic corrected peak area providing an estimate of the (reticular V^{5+})/(reticular V^{4+}) ratio using C_6/A_6 and C_8/A_7 peaks. From LSVs in 0.10 M HCl; $v = 10$ mV/s

lattice that could be adopted without significant structural distortion upon replacement of Zr^{4+} by V^{5+}. Spectral data [8, 9] are in agreement with the foregoing set of considerations.

Conclusions

The reported data support some conclusions:

1. The electrochemistry of vanadium-doped zirconias attached to graphite/polyester composite electrodes can be described in terms of the superimposition of that of finely dispersed vanadium(V) oxide and that of vanadium centers isomorphously substituting Zr^{4+} centers in the zirconia lattice.
2. Electrochemical data indicate that not only V^{4+} but also V^{5+} ions substitute Zr^{4+} ions in the zirconia lattice. The quotient (reticularV^{5+})/(reticular V^{4+}) decreases as the vanadium loading increases.
3. The proportion of vanadium(V) oxide finely dispersed into the zirconia and the total vanadium loading increases as the total amount of vanadium increases above the solubility limit of ca. 5%.
4. The voltammetric response allows discrimination between different structural environments of the vanadium centers. Thus, seven-coordinated V^{5+} ions in monoclinic zirconias exhibit a reduction potential of +0.25 V vs. SCE, while eight-coordinated vanadium ions in tetragonal zirconias are reduced at +0.35 V. The electrochemical oxidation of V^{4+} centers in monoclinic and tetragonal zirconias takes place at +0.47 and +0.41 V, respectively.

Although further research is needed to establish a correlation between structure and electrochemistry, current data illustrate the availability of solid state electrochemistry for providing information on the structure and speciation of new materials. Continuing research is being devoted to the study of the catalytic and electrocatalytic properties of doped zirconias.

References

1. Su SC, Bell AT (1998) J Phys Chem B 102:7000
2. Chen K, Khodakov A, Yang J, Bell AT, Iglesia E (1999) J Catal 186:325
3. Booth FT, Peel GN (1962) Trans Br Ceram Soc 61:359
4. Ren F, Ishida S, Takeuchi N (1999) J Am Ceram Soc 76:1825
5. Tartaj P, Serna CJ, Soria J, Ocaña M (1998) J Mater Res 13:413
6. Monrós G, Carda J, Tena MA, Escribano P, Alarcón J (1991) Trans Br Ceram Soc 90:157
7. Valentín C, Muñoz MC, Alarcón J (1999) J Sol-Gel Sci Technol 15:221
8. Alarcón J (2001) J Mater Sci 36:1189
9. Valentín C, Folgado JV, Alarcón J (2001) Mater Res Bull (in press)
10. Scholz F, Lange B (1993) Trends Anal Chem 11:359
11. Scholz F, Meyer B (1994) Chem Soc Rev 23:341
12. Bruce PG (ed) (1995) Solid state electrochemistry. Cambridge University Press, Cambridge
13. Scholz F, Meyer B (1998) In: Bard AJ, Rubinstein I (eds) Electroanalytical chemistry, vol 20. Dekker, New York, pp 1–87
14. Lamache M, Bauer D (1977) J Electroanal Chem 79:359
15. Livage J (1999) Coord Chem Rev 190–192:391
16. Chirayil T, Zavalij PY, Stanley WM (1998) Chem Mater 10:2629
17. Brainina KZ, Bazarova EV, Volkov VL (1968) Elektrokhimiya 3:69
18. Rozier P, Savariault JM, Galy J (1997) Solid State Ionics 98:133
19. Barrado E, Pardo R, Castrillejo Y, Vega M (1997) J Electroanal Chem 427:35
20. Ryan DM, Riechel TL (1996) Proc Electrochem Soc 96–97:381
21. Friedrich A, Hefele H, Mickler W, Mönner A, Uhlemann E, Scholz F (1998) Electroanalysis 10:244
22. Venkatathri N, Vinod MP, Vijayamohanaan K, Sivasanker S (1996) J Chem Soc Faraday Trans 92:473
23. Privman M, Hepel T (1995) J Electroanal Chem 382:137
24. Privman M, Hepel T (1995) J Electroanal Chem 382:145
25. Eloudseri MM, Vittori O, Durand B (1986) Electrochim Acta 31:1335
26. Newton TN, Baker FB (1964) Inorg Chem 3:569
27. Israel Y, Meites L (1964) J Electroanal Chem 8:99
28. Israel Y, Merits L (1985) In: Bard AJ, Parsons R, Jordon J (eds) Standard potentials in aqueous solutions, chap 17. Dekker, New York
29. Filipovic I, Hahl Z, Gasparac Z, Klemencic V (1954) J Am Chem Soc 76:2074
30. Grygar T (1995) Collect Czech Chem Commun 60:950
31. Grygar T (1995) Collect Czech Chem Commun 60:1261
32. Grygar T (1996) Coll Czech Chem Commun 61:93
33. Grygar T (1996) J Electroanal Chem 405:117
34. Bakardjieva S, Bezdicka P, Grygar T, Vorm P (2000) J Solid State Electrochem 4:306
35. Bodoardo S, Brenet J, Maja M, Spinelli P (1994) Electrochim Acta 39:1999
36. Donne SW, Lawrance GA, Swilkels DAJ (1997) J Electrochem Soc 144:2949
37. Rodrigues S, Munichandraiah N, Shukla AK (1998) J Appl Electrochem 28:1235
38. Bessel CA, Rolison DR (1997) J Phys Chem B 101:1148
39. Dutta PK, Ledney M (1997) Prog Inorg Chem 44:209
40. Wells AF (1978) Structural inorganic chemistry. Oxford University Press, Oxford, pp 464–465